Check for updates

Nonisothermal decomposition and safety parameters of HNIW/TNT cocrystal

Jiao-Qiang Zhang, [ID] *[a] Yun-Long Xu,[a] Qian Jia,[a] Shi-Jie Zhang,[a] Ning Liu, [ID] [b] Hong-Xu Gao[b] and Rong-Zu Hu[b]

To explore the thermal decomposition behavior and evaluate the thermal safety of the cocrystal 2,4,6,8,10,12-hexanitrohexaazaisowurtzitane (HNIW)/2,4,6-trinitrotoluene (TNT), its thermal and kinetic behaviors were studied by differential scanning calorimetry (DSC) technique. With the help of onset temperature (T_e) and maximum peak temperature (T_p) from the non-isothermal DSC curves of HNIW/TNT cocrystal at different heating rates (β), the following were calculated: the value of specific heat capacity (C_p) and the standard molar enthalpy of formation ($\Delta_f H_m^\theta$, s, 298.15 K), the apparent activation energy (E_K and E_O) and pre-exponential constant (A_K) of thermal decomposition reaction obtained by Kissinger's method and Ozawa's method, density (ρ) and thermal conductivity (λ), the decomposition heat (Q_d, as half-explosion heat), Zhang–Hu–Xie–Li's formula, Smith's equation, Friedman's formula, Bruckman–Guillet's formula, Frank-Kamenetskii's formula and Wang–Du's formulas, the values (T_{e0} and T_{p0}) of T_e and T_p corresponding to $\beta \to 0$, thermal explosion temperature (T_{be} and T_{bp}), adiabatic time-to-explosion (t_{tiad}), 50% drop height (H_{50}) for impact sensitivity, critical temperature of hot-spot initiation (T_{cr}), thermal sensitivity probability density function [$S(T)$] vs. temperature (T) relation curves with radius of 1 m and ambient temperature of 300 K, the peak temperature corresponding to the maximum value of $S(T)$ vs. T relation curve ($T_{S(T)max}$), safety degree (SD) and critical ambient temperature (T_{acr}) of thermal explosion. Results show that the kinetic equation describing the exothermic decomposition reaction of HNIW/TNT cocrystal is $d\alpha/dt = \frac{3}{2}(1-\alpha)[-\ln(1-\alpha)]^{\frac{1}{3}}\exp(-2.8318 \times 10^4/T)$. The following thermal safety parameters for the HNIW/TNT cocrystal are obtained: T_{e0} = 464.45 K; T_{p0} = 477.55 K; T_{be} = 472.82 K; T_{bp} = 485.89 K; t_{tiad} = 4.40 s, 4.42 s, and 4.43 s for n = 0, 1, and 2, respectively; T_{cr} = 531.90 K; H_{50} = 19.46 cm; and the values of T_{acr}, $T_{S(T)max}$, SD and P_{TE} are 469.69 K, 470.58 K, 78.57% and 21.43% for sphere; 465.70 K, 470.58 K, 78.17% and 21.83% for infinite cylinder; and 459.39 K, 464.26 K, 77.54% and 22.46% for infinite flat.

1 Introduction

High-density energetic materials (HDEMs) show great potential use in the military field, e.g., as propellants, pyrotechnics, explosives and gas generators.[1–4] Along with the fast development of the energetic materials (EMs), the demand is increasing for the insensitive EMs; specifically, it is necessary to generate high-energy EMs with low sensitivity.[5,6] As is known, the conflicts between increasing chemical energy and decreasing the sensitivity are severe. Many efforts have been made to improve the power and insensitivity of EMs, and synthesis of new compounds and modification of existing materials are the primary methods used.[7–9] Co-crystallization is an effective and convenient means to improve the performance of materials,

and it has drawn wide attention among researchers.[10,11] Co-crystallization, combining two or more neutral molecules through non-covalent interactions, could compromise the merits of the individual substance, and one of the energetic compounds has shown the ability to alter undesirable material properties, such as high sensitivity or low density.[12,13] 2,4,6,8,10,12-Hexanitrohexaazaisowurtzitane (HNIW) is the most powerful explosive owing to its high density (>2.0 g cm^{-3}), good oxygen balance (−10.94%) and high detonation velocity (9400 m s^{-1}), but its high sensitivity toward external stimuli constrains its application.[14] 2,4,6-Trinitrotoluene (TNT) is an extensively used explosive with good stability. Bolton successfully prepared the HNIW·TNT cocrystal (in a 1 : 1 stoichiometry) in 2011,[15] which featured insensitivity and high energy. The nonisothermal decomposition behaviors and thermal safety parameters of EMs play vital roles in theoretical studies and engineering applications, providing significant guidance to their further applications and industrial production. In recent years, reports of the HNIW·TNT cocrystal have been

[a]Key Laboratory of Space Applied Physics and Chemistry of Ministry of Education, Department of Applied Chemistry, School of Science, Northwestern Polytechnical University, Xi'an 710072, China. E-mail: zhangjq@nwpu.edu.cn

[b]Xi'an Modern Chemistry Institute, Xi'an, 710065, China

concentrated on its synthesis, characterization, atomistic simulation and reactive molecular dynamics,[16–22] but there is little literature reported about the thermal behaviors and thermal safety parameters of HNIW·TNT cocrystal. Before HNIW·TNT cocrystal can reach practical application, much work should be done for a more comprehensive understanding of this material. To add to these studies, herein, the non-isothermal decomposition behaviors and detailed thermal safety parameters of HNIW·TNT cocrystal are described. The HNIW·TNT cocrystal was prepared and characterized. Its non-isothermal decomposition was studied by differential scanning calorimetry (DSC), and the thermal safety parameters of HNIW·TNT cocrystal, including the self-accelerating decomposition temperature (T_{SADT}), the critical temperature of thermal explosion (T_b) and the adiabatic time-to-explosion (t_{tiad}), were also calculated with the experimental data from non-isothermal decomposition. Moreover, the 50% drop height of impact sensitivity (H_{50}), the critical temperature of hot-spot initiation caused by impact (T_{cr}), the safety degree (SD), the critical thermal explosion ambient temperature (T_{acr}) and thermal explosion probability (P_{TE}) were also obtained.

2   Experimental

2.1   Caution

General caution: title compound is a hazardous material, explosions of which may occur in certain conditions. Although we had no difficulties during the experiments and in handling the compounds, appropriate safety precautions such as the use of safety glasses, face shields and horn spoons should be taken, especially when the compounds are prepared at a large scale.

2.2   Preparation

HNIW/TNT cocrystal was prepared and purified according to the literature method.[15] It was kept in a vacuum desiccator before use. The structure of HNIW/TNT cocrystal was characterized by infrared spectroscopy (IR) and elemental analysis. IR (KBr): 3111, 3024 (CH), 1599, 1339, 1348, 1259, 943, 885 (NO_2), 1088, 1059 (N–N), 831, 752, 721 (skeleton ring) cm^{-1}. Anal. calcd (%) for $C_{13}H_{11}N_{15}O_{18}$: C 23.47, N 31.58, H 1.67; found (%) C 23.55, N 32.01, H 1.59. High-performance liquid chromatography (HPLC; LC-20AD, Shimadzu Corporation, Japan) was used to confirm the content of HNIW and TNT in the HNIW/TNT cocrystal, with a Phenomenex C_{18} analytical column (5.0 μm, 150 mm × 4.6 mm) at 298.15 K column temperature and the detection wavelength of 254 nm. The results demonstrate that the mole ratio of HNIW to TNT is 1 : 1 in the above prepared HNIW/TNT cocrystal.

2.3   Differential scanning calorimetry

The DSC experiments for the title compound were performed using a Q2000 apparatus (TA, USA) under nitrogen atmosphere at a flow rate of 50 ml min^{-1}. About 0.6 mg of sample was sealed in an aluminum pan, and the heating rates used were 2.5, 5.0, 10.0, 15.0 and 20.0 K min^{-1} from ambient temperature to 773.15 K. DSC curves obtained under the same conditions

overlapped with each other, indicating that the reproducibility of the tests was satisfactory.

3   Results and discussion

3.1   Standard enthalpy of combustion

The standard combustion enthalpy of the title compound, $\Delta_c H_m^\theta$ (HNIW/TNT cocrystal, s, 298.15 K) was derived from the combustion enthalpy change of the following ideal combustion reaction (1) at 298.15 K and 100 kPa,

$$C_{13}H_{11}N_{15}O_{18}(s) + 15.75O_2(g) \rightarrow 13CO_2(g) + 5.5H_2O(l) + 7.5N_2(g), \quad (1)$$
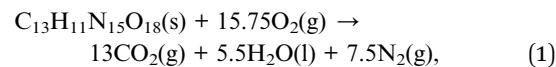
and calculated by Hess's law according to the thermochemical eqn (2),

$$\Delta_c H_m^\theta (\text{HNIW/TNT cocrystal, s, 298.15 K})$$
$$= 13\Delta_f H_m^\theta (CO_2, g, 298.15 \text{ K}) + 5.5\Delta_f H_m^\theta (H_2O, l, 298.15 \text{ K})$$
$$- \Delta_f H_m^\theta (\text{HNIW/TNT cocrystal, s, 298.15 K}), \quad (2)$$
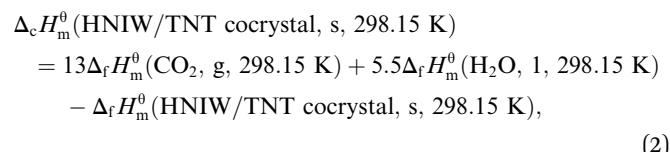
where $\Delta_f H_m^\theta (CO_2, g, 298.15 \text{ K}) = -(393.51 \pm 0.13)$ kJ mol^{-1}, $\Delta_f H_m^\theta (H_2O, l, 298.15 \text{ K})$
$$= -(285.83 \pm 0.042) \text{ kJ mol}^{-1}$$

,[23] and $\Delta_f H_m^\theta$ (HNIW/TNT cocrystal, s, 298.15 K)
$$= 324.445 \pm 0.149 \text{ kJ mol}^{-1},$$

determined through a thermochemical cycle, as reported elsewhere; the result obtained is $-(7012.14 \pm 3.42)$ kJ mol^{-1}.

3.2   Standard energy of combustion

The standard energy of combustion of the title compound $\Delta_c U$ (HNIW/TNT cocrystal, s, 298.15 K) was calculated by the following eqn (4):

$$\Delta_c H_m^\theta (\text{HNIW/TNT cocrystal, s, 298.15 K})$$
$$= \Delta_c U(\text{HNIW/TNT cocrystal, s, 298.15 K}) + \Delta n RT \quad (3)$$
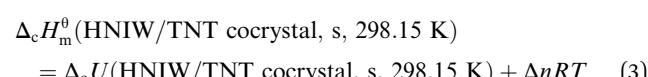
$$\Delta n = n_g \text{ (products)} - n_g \text{ (reactants)} \quad (4)$$

where $\Delta_c H_m^\theta = -(7012.14 \pm 3.42)$ kJ mol^{-1}, n_g is the total amount in mole of gases present as products or as reactants, $\Delta n = 13 + 7.5 - 15.75 = 4.75$, $R = 8.314$ J K^{-1} mol^{-1}, and $T = 298.15$ K. The result is $-(7023.914 \pm 3.42)$ kJ mol^{-1}.

3.3   The nonisothermal decomposition behavior of HNIW/TNT cocrystal

A typical DSC curve at a heating rate of 5.0 K min^{-1} for HNIW/TNT cocrystal is shown in Fig. 1. The curve consists of one endothermic peak and one exothermic peak. The endothermic peak at 413.52 K is the phase change from solid to liquid. The exothermic peak is the decomposition reaction of HNIW/TNT cocrystal; the T_p is 490.61 K, and the T_e is 479.32 K.
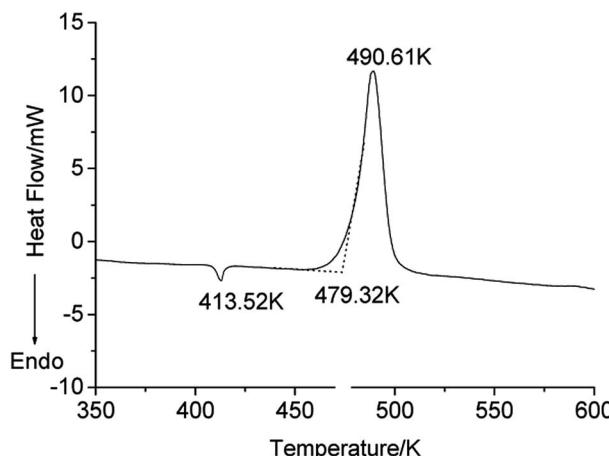
Fig. 1 DSC curve for HNIW/TNT cocrystal at a heating rate of 5.0 K min⁻¹.

3.4 Thermal conductivity (λ)

According to the relationship between specific heat capacity at constant pressure (C_p) and specific heat capacity at constant volume (C_v) as $C_p = 0.83 C_v$[24] and substituting the values of M of 665.32 and a, b, c and d in eqn (5) into eqn (6),

$$C_a H_b O_c N_d = C_{13} H_{11} O_{18} N_{15} \qquad (5)$$

$$C_v = \left\{ \frac{3}{2} \frac{R(a+b+c+d)}{M} \left[1 + \frac{2c^2}{(4a+b)(a+b+c+d)} \right. \right.$$
$$\left. \left. - \frac{2ac^2}{(4a+b)(a+b+c+d)^2} \right] \right\} \qquad (6)$$

we obtain $C_p = 1.01$ J g⁻¹ K⁻¹, which is in accordance with our experiment results, determined by a continuous C_p mode of Micro-DSC III and will be reported elsewhere.

By replacing the values of C_p of 1.01 J g⁻¹ K⁻¹, ρ of 1.844 g cm⁻³, T_m of 413.52 K and M of 665.32 into eqn (7),[25]

$$\lambda = \frac{3.7287 \times 10^{-5} C_p{}^{3.0116} \rho^{0.9279}}{T_m{}^{-0.7652} M^{0.2158}} \qquad (7)$$

the value of λ of 0.168 W (m K)⁻¹ was obtained.

3.5 Explosion properties

By substituting the values of a, b, c and d in $C_a H_b O_c N_d = C_{13} H_{11} O_{18} N_{15}$, $\rho = 1.844$ g cm⁻³, $\Delta_f H_m^\theta = 324.445$ kJ mol⁻¹ into Kamlet–Jacobs eqn (8)–(12),[26] the values of D of 8.624 km s⁻¹, P of 33.89 GPa, N of 0.0289 mol g⁻¹, M_g of 30.34 g mol⁻¹, and Q of 6184.71 J g⁻¹ are obtained.

$$D = 1.01(N M^{1/2} Q^{1/2})^{1/2}(1 + 1.30\rho) \qquad (8)$$

$$P = 1.558 N M^{1/2} Q^{1/2} \rho^2 \qquad (9)$$

$$N = \frac{b + 2d + 2c}{4M} \qquad (10)$$

$$M = \frac{4M}{b + 2c + 2d} \qquad (11)$$

$$Q = 4.184 \times \left(\frac{28.9b + 94.05a + 0.239 \Delta_f H^\theta}{M} \right) \times 10^{-3} \qquad (12)$$

where D is detonation velocity (km s⁻¹), P detonation pressure (GPa), N moles of gas detonation products per gram of explosive, M average molecular weight of gaseous products, Q chemical energy of detonation (J g⁻¹), ρ density of explosives (g cm⁻³), and $\Delta_f H^\theta$ standard enthalpy of formation.

By substituting the values of $x_{N_2} = 7.5$, $x_{H_2O} = 5$, $x_{CO_2} = 6$, $x_{CO} = 1$, $x_{H_2} = 0.5$, $x_{O_2} = 0$, $x_C = 6$, and $M = 665.32$ g mol⁻¹ from reaction formula (13) and $\rho = 1.884$ g cm⁻³ into empirical nitrogen equivalent eqn (14) and (15) (ref. 24) for predicting the D and P of C–H–N–O explosives, the values of D of 8.646 km s⁻¹ and P of 33.76 GPa are obtained.

$$C_{13}H_{11}N_{15}O_{18}(s) \rightarrow 6CO_2 + 5H_2O + \frac{1}{2}H_2$$
$$+ CO + 7.5N_2 + 6C \qquad (13)$$
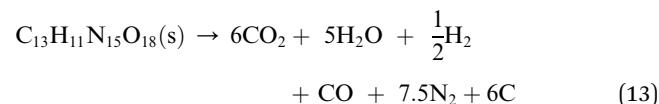
$$D = \frac{100}{M}(695 + 1150\rho)(1.00 x_{N_2} + 0.64 x_{H_2O} + 1.34 x_{CO_2}$$
$$+ 0.72 x_{CO} + 0.18 x_{H_2} + 0.50 x_{O_2} + 0.12 x_C) \qquad (14)$$

where 695 and 1150 are constants; 1.00, 0.64, 1.34, 0.72, 0.18, 0.50, and 0.12 are the nitrogen equivalent coefficients of gaseous detonation products N_2, H_2O, CO_2, CO, H_2, O_2, C of the explosive.

Furthermore,

$$P = 1.060 \left[\rho \frac{100}{M}(1.000 x_{N_2} + 0.64 x_{H_2O} + 1.34 x_{CO_2} \right.$$
$$\left. + 0.72 x_{CO} + 0.18 x_{H_2} + 0.50 x_{O_2} + 0.12 x_C) \right]^2 - 0.619 \qquad (15)$$

where 1.060 and 0.619 are constants. The abovementioned calculation results show that HNIW/TNT cocrystal has an explosion performance level approaching those of HMX and RDX [D (HMX) = 8.92 km s⁻¹ (β = 1.844 g cm⁻³), P (HMX) = 35.72 GPa and D (RDX) = 8.67 km s⁻¹ (β = 1.765 g cm⁻³), P (RDX) = 32.97 GPa], obtained using Kamlet–Jacobs equations.

3.6 Analysis of kinetic data for the main exothermic decomposition reaction of HNIW/TNT cocrystal

Two isoconversional methods [eqn (16) and (17)] were used to obtain the kinetic parameters (the apparent activation energy (E_a) and pre-exponential constant (A)) of the main exothermic decomposition reaction for the title compound:

Differential method. Kissinger equation[27]

$$\ln\left(\frac{\beta_i}{T_{pi}{}^2}\right) = \ln\frac{A_K R}{E_K} - \frac{E_K}{R}\frac{1}{T_{pi}} \qquad (16)$$

Integral method. Ozawa equation[28]

$$\lg \beta_i = \lg\left[\frac{A_k E_{oe(or\ op)}}{RG(\alpha)}\right] - 2.315 - 0.4567\frac{E_{oe(or\ op)}}{RT_{o(or\ p)i}} \quad (17)$$

where α is the degree of reaction, T the absolute temperature, E the apparent activation energy, β the heating rate, R the gas constant, T_p the DSC curve peak temperature, and A the pre-exponential factor.

From the original data in Table 1, E_K obtained by Kissinger's method[27] is determined to be 239.40 kJ mol^{-1}. The pre-exponential constant (A) is $10^{23.50}$ s^{-1}. The linear correlation coefficient (r_K) is 0.9969. The value of E_o obtained by Ozawa's method[28] is 235.45 kJ mol^{-1}. The value of r_0 is 0.9971. The value of E_{eo} obtained by T_{ei} vs. β_i relation is 222.08 kJ mol^{-1}. The value of r_{eo} is 0.9946.

By substituting the experimental data, β_i, T_i and α_i, $i = 1, 2, \dots n$, listed in Table 2 from DSC curves at differential heating rates into eqn (18), the values of E_α for any given value of α were obtained and are shown in Fig. 2. The average value of E_α in the α range of 0.10 to 0.90 in Fig. 2 is in good agreement with the calculated values obtained by Kissinger's method and Ozawa's method. The E values calculated using eqn (18)[29] are used to check the validity of activation energy by the other methods.

$$\Omega_{1I}(E_\alpha) = \min\left|\sum_{i=1}^{n}\sum_{j\neq i}^{n}\frac{\beta_j I(E_\alpha, T_{\alpha,i})}{\beta_i I(E_\alpha, T_{\alpha,j})} - n(n-1)\right| \quad (18)$$

where the $I(E_\alpha, T_\alpha)$ integral is obtained taking the Senum–Yang approximation calculation for approximation of 3rd degree: $I_{SY-3}(E, T) = \left[Te^{-u}\left(\frac{u^2 + 10u + 18}{u^3 + 12u^2 + 36u + 24}\right)\right]$ where $u = E/RT$.

The data (β, T_i, α_i, $i = 1, 2, \dots$) in the range of $\alpha = 0.10$–0.90 and 47 kinetic model functions[29] were input to following eqn (19)–(23) to obtain the values of E and A from a single non-isothermal DSC curve.

Ordinary-integral equation[30]

$$\ln\left[\frac{G(\alpha)}{T^2}\right] = \ln\left[\frac{AR}{\beta E}\left(1 - \frac{2RT}{E}\right)\right] - \frac{E}{RT} \quad (19)$$

Universal integral equation[31]

$$\ln\left[\frac{G(\alpha)}{T - T_0}\right] = \ln\frac{A}{\beta} - \frac{E}{RT} \quad (20)$$

MacCall–Tanner equation[32]

$$\log[G(\alpha)] = \log\left(\frac{AE}{\beta R}\right) - 0.4828E^{0.4357} - \frac{0.449 + 0.217E}{0.001}\frac{1}{T} \quad (21)$$

Table 1 Maximum peak temperature (T_p) and onset temperature (T_e) of the exothermic decomposition reaction for HNIW/TNT cocrystal determined by the DSC curves at various heating rates (β)

β/(K min^{-1})	2.5	5.0	10.0	15.0	20.0
T_p/K	484.83	490.61	495.40	498.75	502.39
T_e/K	472.65	479.32	483.50	486.82	490.59

Table 2 Data for HNIW/TNT cocrystal determined by DSC at different heating rates and apparent activation energies (E_α) of thermal decomposition obtained by integral isoconversional non-linear (NL-INT) method[a]

	T_i/(K)						
α/(%)	2.5	5.0	10.0	15.0	20.0	E_α/kJ mol^{-1}	min
0.0	452.38	461.70	464.54	467.25	470.47	203.64	0.6861
2.5	465.87	472.91	478.00	481.57	484.98	202.94	0.0659
5.0	469.08	475.84	481.08	484.73	488.22	205.02	0.0518
7.5	471.12	477.79	483.11	486.79	490.32	205.97	0.0479
10.0	472.67	479.29	484.65	488.34	491.87	207.17	0.0454
12.5	473.93	480.52	485.88	489.57	493.12	208.40	0.0461
15.0	474.99	481.57	486.91	490.60	494.14	209.78	0.0464
17.5	475.91	482.49	487.79	491.48	495.01	211.20	0.0479
20.0	476.72	483.30	488.57	492.25	495.77	212.53	0.0489
22.5	477.46	484.03	489.25	492.93	496.44	214.05	0.0508
25.0	478.13	484.68	489.87	493.54	497.05	215.40	0.0522
27.5	478.74	485.28	490.44	494.11	497.62	216.46	0.0537
30.0	479.31	485.84	490.97	494.63	498.14	217.63	0.0552
32.5	479.84	486.35	491.46	495.13	498.63	218.55	0.0555
35.0	480.35	486.83	491.93	495.59	499.10	219.51	0.0563
37.5	480.82	487.28	492.38	496.04	499.56	220.07	0.0568
40.0	481.27	487.71	492.81	496.48	500.00	220.56	0.0567
42.5	481.69	488.12	493.23	496.91	500.44	220.68	0.0567
45.0	482.11	488.51	493.64	497.34	500.87	220.83	0.0556
47.5	482.50	488.89	494.04	497.76	501.30	220.65	0.0553
50.0	482.88	489.25	494.44	498.18	501.72	220.38	0.0533
52.5	483.25	489.62	494.84	498.59	502.15	219.98	0.0531
55.0	483.61	489.98	495.23	499.01	502.57	219.50	0.0520
57.5	483.97	490.34	495.63	499.42	502.99	219.05	0.0507
60.0	484.32	490.70	496.02	499.84	503.42	218.37	0.0502
62.5	484.67	491.05	496.42	500.26	503.85	217.65	0.0487
65.0	485.01	491.42	496.82	500.68	504.28	216.91	0.0481
67.5	485.36	491.78	497.23	501.11	504.72	216.10	0.0466
70.0	485.71	492.16	497.65	501.54	505.17	215.29	0.0460
72.5	486.06	492.55	498.08	501.99	505.63	214.35	0.0449
75.0	486.43	492.95	498.53	502.45	506.11	213.45	0.0438
77.5	486.82	493.38	498.99	502.93	506.60	212.26	0.0432
80.0	487.24	493.83	499.48	503.44	507.12	211.94	0.0422
82.5	487.69	494.31	500.00	503.98	507.68	211.14	0.0418
85.0	488.18	494.84	500.56	504.56	508.28	210.41	0.0418
87.5	488.73	495.44	501.19	505.21	508.94	209.74	0.0412
90.0	489.38	496.14	501.92	505.97	509.70	209.12	0.0402
92.5	490.18	496.99	502.82	506.88	510.62	208.54	0.0387
95.0	491.29	498.14	504.02	508.10	511.81	208.50	0.0355
97.5	493.12	500.07	506.03	510.06	513.64	209.70	0.0271
100	502.27	509.77	519.78	524.06	523.51	183.13	0.4347

[a] α is the degree of reaction; T_i is the corresponding temperature at different heating rates for different α; min is the minimum value of eqn (18) for any given value of α.

Satava–Sestak equation[33]

$$\log G(\alpha) = \log\frac{A_s E_s}{R\beta} - 2.315 - 0.4567\frac{E_s}{RT} \quad (22)$$

Agrawal equation[34]

$$\ln\left[\frac{G(\alpha)}{T^2}\right] = \ln\left\{\frac{AR}{\beta E}\left[\frac{1 - 2\left(\dfrac{RT}{E}\right)}{1 - 5\left(\dfrac{RT}{E}\right)^2}\right]\right\} - \frac{E}{RT} \quad (23)$$
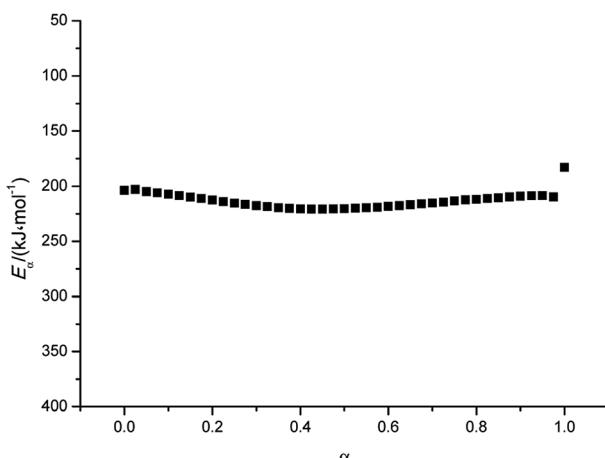
Fig. 2 The E_α–α curve obtained by Ozawa's method.

where $G(\alpha)$ is the integral model function, respectively, T the temperature (K) at time t, α the degree of reaction, and R the gas constant.

The kinetic parameters obtained by the logical choice method[31] are presented in Table 3. Their values for E are very close to each other. The values of E_a and A obtained from a single non-isothermal DSC curve are in good agreement with the calculated values obtained by Kissinger's method and Ozawa's method. Therefore, we conclude that the reaction mechanism of the main exothermic decomposition process of the title compound is classified as $G(\alpha) = [1 - \ln(1 - \alpha)]^{2/3}$, $f(\alpha) = \frac{3}{2}(1 - \alpha)[-\ln(1 - \alpha)]^{\frac{1}{3}}$. Substituting $f(\alpha)$ with $f(\alpha) = \frac{3}{2}(1 - \alpha)[-\ln(1 - \alpha)]^{\frac{1}{3}}$, E with 235.44 kJ mol^{-1} and A with $10^{23.50}$ s^{-1} in eqn (24):

$$\frac{d\alpha}{dt} = Af(\alpha)\exp(-E/RT) \quad (24)$$

the kinetic equation of the exothermic decomposition reaction of HNIW/TNT cocrystal may be described as:

$$d\alpha/dt = 10^{23.50} f(\alpha)$$
$$= \frac{3}{2}(1 - \alpha)[-\ln(1 - \alpha)]^{\frac{1}{3}}\exp\left(-2.8318 \times 10^4/T\right) \quad (25)$$

3.7 Heat-temperature quotient for the exothermic decomposition of HNIW/TNT cocrystal

The exothermic peak in Fig. 1 is caused by the decomposition reaction. Heat-temperature quotient ΔS_d of the process equals to:

$$\Delta S_d = Q_d/T_{p0} = -(-2057.41 \text{ kJ mol}^{-1})/$$
$$477.55 \text{ K} = 4.308 \text{ kJ mol}^{-1} \text{ K}^{-1} \quad (26)$$

In eqn (26), Q_d is the heat of decomposition reaction, which is defined as $Q_d = 0.5Q$, i.e., Q_d is the half-chemical energy (heat) of detonation. For HNIW/TNT cocrystal, $Q_d = 0.5Q =$

3092.36 J g^{-1}, and T_{p0} is the peak temperature T_p corresponding to $\beta \to 0$.

3.8 Self-accelerating decomposition temperature T_{SADT}

Setting T_e as the onset temperature and T_p as the peak temperature, and defining $T_{e0 \text{ or } p0}$ as the value of $T_{(e0 \text{ or } p0)i}$ corresponding to $\beta \to 0$ and T_{e0} as the self-accelerating decomposition temperature T_{SADT}, we have:

$$T_{e \text{ or } p} = T_{e0 \text{ or } p0} + b\beta_i + c\beta_i^2 + d\beta_i^3, i = 1, 2, ..., L \quad (27)$$

and

$$T_{e0} = T_{SADT} \quad (28)$$

Replacing the experimental data: β_i, T_{ei}, T_{pi}, $i = 1, 2, ..., 5$ in Table 1 into eqn (27), the values of T_{e0} of 464.45 K and T_{p0} of 477.55 K are obtained. The T_{SADT} value of 464.45 K is obtained by eqn (28).

3.9 The critical temperature of thermal explosion (T_b)

The critical temperature of thermal explosion (T_b) is an important parameter in evaluating the safety and elucidating transition tendency from thermal decomposition to thermal explosion for small-scale EMs.

For HNIW/TNT cocrystal, the values of T_b obtained by the Zhang–Hu–Xie–Li equation [eqn (29)] taken from ref. 35 using the values of T_{e0} (464.45 K) and T_{p0} (477.55 K) and the values of E_{oe} (222.08 kJ mol^{-1}) and E_{op} (235.45 kJ mol^{-1}) are 472.82 and 485.89 K, respectively:

$$T_{be0(\text{or bp0})} = \frac{E_{oe \text{ or op}} - \sqrt{E_{oe \text{ or op}}^2 - 4E_{oe \text{ or op}}RT_{e0(\text{or p0})}}}{2R} \quad (29)$$

In comparison with RDX for $T_{bp} = 454.08$ K,[25] the high value of T_b shows that it is difficult for the transition from thermal decomposition to thermal explosion to take place.

3.10 Thermodynamic parameters of activation reaction

The entropy of activation ($\Delta S^{\neq}$), enthalpy of activation ($\Delta H^{\neq}$), and Gibbs free energy of activation ($\Delta G^{\neq}$) corresponding to $T = T_{p0} = 477.55$ K, $E = E_K = 239\,400$ J mol^{-1}, and $A = A_K = 10^{23.50}$ obtained by eqn (30)–(32) are 192.74 J mol^{-1} K^{-1}, 235.43 kJ mol^{-1} and 143.39 kJ mol^{-1}, respectively. The positive value of $\Delta G^{\neq}$ indicates that the exothermic decomposition reaction for HNIW/TNT cocrystal must proceed under the heating condition.

$$A e^{-E/RT} = \frac{k_B T}{h} e^{-\frac{\Delta G^{\neq}}{RT}} \quad (30)$$

$$\Delta H^{\neq} = E - RT \quad (31)$$

$$\Delta G^{\neq} = \Delta H^{\neq} - T\Delta S^{\neq} \quad (32)$$

where k_B is the Boltzmann constant (1.3807×10^{-23} J K^{-1}) and h is the Planck constant (6.626×10^{-34} J s).

Table 3 Thermokinetic parameters for thermal decomposition process of HNIW/TNT cocrystal for $G(\alpha) = [1 - \ln(1 - \alpha)]^{2/3}$, $f(\alpha) = \dfrac{3}{2}(1 - \alpha)[-\ln(1 - \alpha)]^{\frac{1}{3}a}$

Method	β/K min^{-1}	E/kJ mol^{-1}	lg(A_0/s^{-1})	r	Q
Ordinary-integral equation[30]	2.5	231.87	22.69	0.9998	0.0028
	5.0	238.46	23.37	0.9998	0.0045
	10.0	236.01	23.13	0.9991	0.0162
	15.0	233.85	22.87	0.9986	0.0256
	20.0	234.05	22.83	0.9982	0.0336
Universal integral method[31]	2.5	235.87	21.35	0.9998	0.0043
	5.0	242.52	22.02	0.9998	0.0045
	10.0	240.20	21.79	0.9992	0.0161
	15.0	237.98	21.53	0.9987	0.0255
	20.0	238.21	21.50	0.9983	0.0335
Maccall–Tanner[32]	2.5	232.93	22.80	0.9998	0.0008
	5.0	239.68	23.50	0.9998	0.0008
	10.0	238.68	23.49	0.9998	0.0008
	15.0	235.19	23.01	0.9987	0.0048
	20.0	235.45	22.98	0.9983	0.0063
Satava–Sestak equation[33]	2.5	228.11	22.34	0.9998	0.0008
	5.0	234.48	23.00	0.9998	0.0008
	10.0	237.39	23.26	0.9992	0.0030
	15.0	230.24	22.54	0.9987	0.0048
	20.0	230.49	22.51	0.9983	0.0063
Agrawal[34]	2.5	231.87	22.69	0.9998	0.0043
	5.0	238.46	23.36	0.9998	0.0045
	10.0	236.10	23.13	0.9991	0.0162
	15.0	233.85	22.87	0.9986	0.0256
	20.0	234.05	22.83	0.9982	0.0336
Mean		235.44	22.70		
Kissinger[27]		239.40	23.50	0.9969	
Flynn–Wall Ozawa[28]		235.45		0.9971	

^{a} β is the heating rate; E is the activation energy; A_0 is the pre-exponential constant; r is the linear correlation coefficient; Q is the variance.

3.11 The determination of the adiabatic time-to-explosion

The adiabatic time-to-explosion (t_{tiad}, s) of energetic materials is the time of energetic material thermal decomposition transitioning to explosion under adiabatic conditions, and it is an important parameter for assessing the thermal stability and the safety of energetic materials. The estimation formulae used to calculate the adiabatic time-to-explosion (t) of energetic materials are Smith's eqn (33)–(35) taken from ref. 36.

$$C_p \frac{dT}{dt} = QA \exp(-E/RT) f(\alpha) \tag{33}$$

$$\alpha = \int_{T_0}^{T} \frac{C_p}{Q} dT \tag{34}$$

$$t = \frac{1}{QA} \int_{T_0}^{T} \frac{C_p \exp(E/RT)}{f(\alpha)} dT \tag{35}$$

where C_p is the specific heat capacity (J g^{-1} K^{-1}); $f(\alpha)$ is the differential mechanism function; E is the apparent activation energy; A is the pre-exponential constant; Q is the heat of decomposition; R is the gas constant (8.314 J mol^{-1} K^{-1}); and α is the conversion degree.

By substituting the original data of $C_p = 1.01$ J g^{-1} K^{-1}, $f(\alpha) = (1 - \alpha)^n$, $E = 239\,400$ J mol^{-1}, $A = 10^{23.50}$ s^{-1}, $Q_d = 3092.36$ J g^{-1}, and $R = 8.314$ J mol^{-1} K^{-1}, the integral upper limit $T = T_b = 472.82$ K and the lower limit $T_0 = T_{e0} = 464.45$ K into eqn (35), the values of t of 4.40 s for $n = 0$, 4.42 s for $n = 1$, and 4.43 s for $n = 2$ are obtained.

3.12 The critical temperature of hot-spot initiation (T_{cr})

The interior of energetic materials (EMs) could create a local thermal point when the EMs accept energy, and the EMs will explode from thermal decomposition when the hot-spot temperature reaches the explosive temperature. The critical temperature of hot-spot initiation (T_{cr}) is an important parameter for evaluating the thermal safety of EMs.

By submitting the density $\rho = 1.844$ g cm^{-3} of HNIW/TNT cocrystal, specific heat capacity $C_p = 1.01$ J g^{-1} K^{-1}, thermal conductivity $\lambda = 16.8 \times 10^{-4}$ J cm^{-1} s^{-1} K^{-1}, heat of decomposition $Q_d = 3092.36$ J g^{-1}, kinetic parameters $E = 239\,400$ J mol^{-1} and $A = 10^{23.50}$ s^{-1}, $T_{\text{room}} = 293.15$ K, $R = 8.314$ J mol^{-1} K^{-1}, hot-spot critical radius $a = 10^{-3}$ cm (ref. 36) and time interval $t - t_0 = 10^{-4}$ s (ref. 37) to Bruckman–Guillet's first-order estimation equation [eqn (36)],[38,39] the value of $T_{\text{cr,hotspot}}$ of 258.75 °C (531.90 K) is obtained.

$$\left(\frac{4}{3}\pi a^3\right)\rho Q_\text{d}\left\{1 - \exp\left[-(t - t_0)A\text{e}^{-E/RT_\text{cr}}\right]\right\}$$

$$= \int_a^\infty 4\pi r^2 \rho c_\text{p}\left[\frac{a\theta_0}{r}\,\text{erfc}\left[\frac{r - a}{2\sqrt{Bt}}\right]\right]\text{d}r$$

$$= \int_a^\infty 4\pi r^2 \rho c_\text{p}\left[\frac{a(T_\text{cr,hotspot} - T_\text{room})}{r}\,\text{erfc}\left[\frac{r - a}{2\sqrt{\dfrac{\lambda}{\rho c_\text{p}}t}}\right]\right]\text{d}r \quad (36)$$

3.13   50% drop height (H_{50}) impact sensitivity

Impact sensitivity is an important parameter for evaluating the security and reliability of EMs and can be characterized by 50% drop height (H_{50}). Using data of $\lambda = 16.80 \times 10^{-4}$ J cm^{-1} s^{-1} K^{-1}, $\rho = 1.844$ g cm^{-3}, $Q_\text{d} = 3146.89$ J g^{-1}, $E = 239\,400$ J mol^{-1}, and $A = 10^{23.50}$ s^{-1}, the H_{50} of HNIW/TNT cocrystal was estimated as 19.46 cm by Friedman's formula (eqn (37)).[40,41] This value shows that it has impact sensitivity level approaching those of PETN (15.6 cm) and tetryl (17.6 cm)[37]

$$0.282312\,\lg(H_{50}) + \lg\sqrt{\frac{\lambda}{A\rho Q_\text{d}}} - 0.347174$$

$$+ \frac{0.02612E}{T_1 + 33.8765H_{50}^{0.564623}} = 0 \quad (37)$$

3.14   Critical thermal explosion ambient temperature T_acr, thermal sensitivity probability density function $S(T)$, safety degree SD and thermal explosion probability P_TE

To explore the heat resistance of HNIW/TNT cocrystal, the values of T_acr, $S(T)$ *vs.* T relation, SD and P_TE are calculated by Frank-Kamenetskii (38)[42] and Wang–Du's formulas (39)–(42).[43] In formulas (38)–(44), T_acr is the critical thermal explosion ambient temperature in K; E is the activation energy in J mol^{-1}; A is the pre-exponential constant in s^{-1}; R is the gas constant in 8.314 J K^{-1} mol^{-1}; λ is the thermal conductivity in W m^{-1} K^{-1}; δ is the Frank-Kamenetskii parameter (FK); δ_cr is the criticality of thermal explosion of exothermic system; r is characteristic measurement of reactant in m; Q_d is decomposition heat in J kg^{-1}; ρ is density in kg m^{-3}; μ_T is the average value of temperature, K; σ_δ is the standard deviation of FK parameter; σ_T is the standard deviation of ambient temperature; T is surrounding temperature; $S(T)$ is the thermal sensitivity probability density function; SD is safety degree; and P_TE is thermal explosion probability.

$$T_\text{acr} = \frac{-E_\text{K}}{2R\,\text{Lambert}\,W_{-1}\left[-\dfrac{1}{2}\sqrt{\dfrac{\lambda E_\text{K}\delta_\text{cr}}{r^2 Q_\text{d}\rho A_\text{K}R}}\right]} \quad (38)$$

$$S(T) = \frac{W(E_\text{K} - 2RT)}{\sqrt{2\pi}\sigma_\delta RT^4}$$

$$\times\exp\left\{-\left[W\frac{\exp\left(-\dfrac{E_\text{K}}{RT}\right)}{T^2} - \delta_\text{cr}\right]^2\middle/2\sigma_\delta{}^2 - \frac{E_\text{K}}{RT}\right\} \quad (39)$$

where:

$$\frac{r^2 Q_\text{d}E_\text{K}\rho A_\text{K}}{\lambda R} = W \quad (40)$$

$$\sigma_\delta = W\left(\frac{E_\text{K} - 2R\mu_\text{T}}{R\mu_\text{T}{}^4}\right)\exp\left(-\frac{E_\text{K}}{R\mu_\text{T}}\right)\sigma_\text{T} \quad (41)$$

$$\mu_\text{T} = \frac{-E_\text{K}}{2R\,\text{Lambert}\,W_{-1}\left(-\dfrac{1}{2}\sqrt{\dfrac{\lambda E_\text{K}\delta_\text{cr}}{r^2 Q_\text{d}\rho A_\text{K}R}}\right)} \quad (42)$$

and σ_δ is the standard derivation of the Frank-Kamenetskii parameter, σ_T is the standard derivation of the measured surrounding temperature, and μ_T is the mean value of T.

SD was obtained by eqn (43):

$$\text{SD} = \int_0^{+\infty}\int_0^{+\infty}\frac{W(E_\text{K} - 2RT)}{2\pi\sigma_\delta\sigma_\text{T}RT^4}\exp$$

$$\left\{-\left[W\frac{\exp\left(-\dfrac{E_\text{K}}{RT}\right)}{T^2} - \delta_\text{cr}\right]^2\middle/2\sigma_\delta{}^2 - \frac{E_\text{K}}{RT} - \frac{(Y - T + \mu_\text{T})^2}{2\sigma_\text{T}{}^2}\right\}\text{d}T\text{d}Y \quad (43)$$

The thermal explosion probability (P_TE) is expressed as eqn (44):

$$P_\text{TE} = 1 - \text{SD} \quad (44)$$
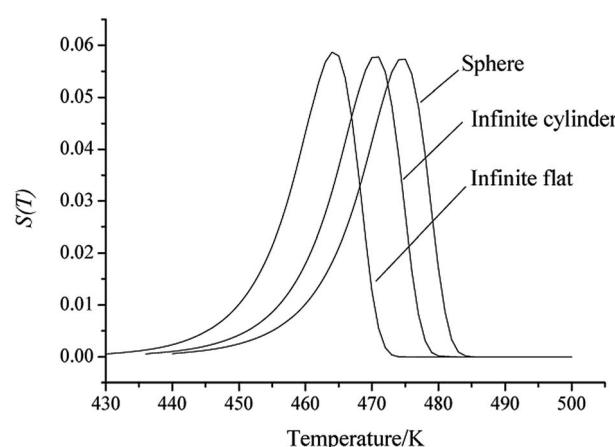
Fig. 3   The $S(T)$ *vs.* T relation curves for infinite flat like, infinite cylindrical and spherical HNIW/TNT cocrystal.

Table 4 Results for the determination of thermal sensitivity for the HNIW/TNT cocrystal[a]

Shape types of reactant	W/K^2	T_{arc}/K	σ_T/K	$T_{S(T)max}/\mathrm{K}$	$S(x)_{TP}$	SD/%	$P_{TE}/\%$
1	3.091×10^{32}	469.69	4.19	470.58	0.0581	78.57	21.43
2	3.091×10^{32}	465.70	2.57	470.58	0.0581	78.17	21.83
3	3.091×10^{32}	459.39	1.16	464.26	0.0581	77.54	22.46

[a] 1 is the sphere; 2 is the infinite cylinder; 3 is the infinite flat.

By substituting the values of $r = 1$ m, $Q_d = 3.09236 \times 10^6$ J kg^{-1}, $E = 239\,400$ J mol^{-1}, $A = 10^{23.50}$ s^{-1}, $\rho = 1.844 \times 10^3$ kg m^{-3}, $\lambda = 0.168$ W m^{-1} K^{-1}, ambient temperature $T_a = 400$ K, $\sigma_\delta = 10$ K into eqn (39)–(42), the $S(T)$ *vs.* T relation curves for infinite flat, infinite cylindrical and spheroid HNIW/TNT cocrystal (Fig. 3) and thermal sensitivity of the HNIW/TNT cocrystal (Table 4) are obtained, showing that the accelerating tendency from adiabatic decomposition to explosion of large-scale HNIW/TNT cocrystal and the thermal safety of HNIW/TNT cocrystal with different shapes decreases in the order: sphere > infinite cylinder > infinite flat.

4 Conclusions

[1] The thermodynamic data describing the energetic characteristics of HNIW/TNT cocrystal are presented: (a) $\Delta_c H_m^\theta$(HNIW/TNT cocrystal, s, 298.15 K) $= -(7012.14 \pm 3.42)$ kJ mol^{-1}; (b) $\Delta_c U$ (HNIW/TNT cocrystal, s, 298.15 K) $= -(7023.91 \pm 3.40)$ kJ mol^{-1}; (c) chemical energy of detonation $Q = 6184.71$ J g^{-1}.

[2] The nonisothermal thermal safety data used to evaluate the heat resistance and the transition resistance from thermal decomposition to thermal explosion of small-scale HNIW/TNT cocrystal and faster select samples are presented: $T_{e0} = 464.45$ K, $T_{p0} = 477.55$ K, $T_{be} = 472.82$ K, $T_{bp} = 485.89$ K, $t_{tiad} = 4.40$ s for $n = 0$, $t_{tiad} = 4.42$ s for $n = 1$, $t_{tiad} = 4.43$ s for $n = 2$, $T_{cr} = 531.90$ K, $H_{50} = 19.46$ cm.

[3] The exothermic decomposition reaction of HNIW/TNT cocrystal can be described by the kinetic equation: $d\alpha/dt = 10^{23.50} f(\alpha) = \frac{3}{2}(1-\alpha)[-\ln(1-\alpha)]^{\frac{1}{3}}\exp(-2.8318 \times 10^4/T)$.

[4] HNIW/TNT cocrystal is sensitive to impact; the value of H_{50} is 19.46 cm, which is better than PETN ($H_{50} = 15.6$ cm) and tetryl ($H_{50} = 17.6$ cm).

[5] The values of T_{acr}, $T_{S(T)max}$, SD and P_{TE} are 469.69 K, 470.58 K, 78.57% and 21.43% for sphere; 465.70 K, 470.58 K, 78.17% and 21.83% for infinite cylinder; and 459.39 K, 464.26 K, 77.54% and 22.46% for infinite flat. The thermal safety of large-scale HNIW/TNT cocrystal with different shapes decreases in the order: sphere > infinite cylinder > infinite flat.

[6] HNIW/TNT cocrystal has a high standard molar enthalpy of formation, high standard combustion energy, and high chemical energy (heat) of detonation, better thermal safety, an explosion performance level approaching those of HMX and RDX, and impact sensitivity level approaching those of PETN and tetryl and can be used as a main ingredient of composite explosive.

Conflicts of interest

There are no conflicts to declare.

References

1 Q. H. Zhang and J. N. M. Shreeve, *Angew. Chem., Int. Ed.*, 2014, **53**(10), 2540–2542.
2 S. B. Kim, K. J. Kim, M. H. Cho, J. H. Kim, K. T. Kim and S. H. Kim, *ACS Appl. Mater. Interfaces*, 2016, **8**(14), 9405–9412.
3 Q. H. Lin, Y. C. Li, C. Qi, W. Liu, Y. Wang and S. P. Pang, *J. Mater. Chem. A*, 2013, **1**(23), 6776–6785.
4 X. X. Zhao, S. H. Li, Y. Wang, Y. C. Li, F. Q. Zhao and S. P. Pang, *J. Mater. Chem. A*, 2016, **4**(15), 5495–5504.
5 C. He, J. Zhang, D. A. Parrish and J. N. M. Shreeve, *J. Mater. Chem. A*, 2013, **1**(8), 2863–2868.
6 V. Thottempudi, J. H. Zhang, C. L. He and J. N. M. Shreeve, *RSC Adv.*, 2014, **4**(92), 50361–50364.
7 Y. R. Yao, X. Chen, Y. P. Hu, B. Yan, Y. L. Guan, J. R. Song and H. X. Ma, *J. Chem. Thermodyn.*, 2017, **104**, 67–72.
8 C. An, J. Wang, W. Xu and F. Li, *Propellants, Explos., Pyrotech.*, 2010, **35**(4), 365–372.
9 X. Wang, K. Xu, Q. Sun, B. Wang, C. Zhou and F. Zhao, *Propellants, Explos., Pyrotech.*, 2015, **40**(1), 9–12.
10 F. Laraochoa and G. Espinosapérez, *Supramol. Chem.*, 2007, **19**(8), 553–557.
11 C. Hong, Y. Xie, Y. Yao, G. Li, X. Yuan and H. Shen, *Pharm. Res.*, 2015, **32**(1), 47–60.
12 J. C. Bennion, Z. R. Siddiqi and A. J. Matzger, *Chem. Commun.*, 2017, **53**(45), 6065–6068.
13 J. Tao, B. Jin, S. Chu, R. Peng, Y. Shang and B. Tan, *RSC Adv.*, 2018, **8**(4), 1784–1790.
14 Y. Wang, Z. Yang, H. Li, X. Zhou, Q. Zhang, J. Wang and Y. Liu, *Propellants, Explos., Pyrotech.*, 2014, **39**(4), 590–596.
15 O. Bolton and A. J. Matzger, *Angew. Chem.*, 2011, **123**, 9122–9125.
16 H. Lin, J. F. Chen, S. G. Zhu, H. Z. Li and Y. Huang, *J. Energ. Mater.*, 2016, **35**(1), 95–108.
17 H. Liu, Z. Yang and Y. H. He, *Chin. J. Explos. Propellants*, 2017, **40**(1), 14–20.

18 Z. W. Yang, H. Huang, H. Z. Li, X. Q. Zhou, J. S. Li and F. D. Nie, *Chin. J. Explos. Propellants*, 2012, **20**(2), 256–257.

19 H. Li, Y. Shu, S. Gao, L. Chen, Q. Ma and X. Ju, *J. Mol. Model.*, 2013, **19**(11), 4909–4917.

20 C. L. Wu, S. H. Zhang, R. J. Gou, F. D. Ren, G. Han and S. F. Zhu, *Comput. Theor. Chem.*, 2018, **1127**, 22–30.

21 D. Guo, Q. An, S. V. Zybin, W. A. Goddard III, F. L. Huang and B. Tang, *J. Mater. Chem. A*, 2015, **3**(10), 5409–5419.

22 D. Z. Guo, Q. An, W. A. Goddard III, S. V. Zybin and F. L. Huang, *J. Phys. Chem. C*, 2014, **118**(51), 30202–30208.

23 J. D. Cox, D. D. Wagman and V. A. Medvedev, *CODATA Key Values for Thermodynamics*, Hemisphere Pub. Corp., 1989.

24 R. Z. Hu, E. G. Yao, H. X. Ma, H. Zhang, H. X. Gao, L. Han, F. Q. Zhao, Y. Luo and H. A. Zhao, *Chin. J. Energ. Mater.*, 2015, **23**(12), 1243–1244.

25 R. Z. Hu, F. Q. Zhao, H. X. Gao, H. X. Ma, H. Zhang, K. Z. Xu, H. A. Zhao and E. G. Yao, *Acta Phys.–Chim. Sin.*, 2013, **29**(10), 2071–2078.

26 M. J. Kamlet and S. J. Jacobs, *J. Chem. Phys.*, 1968, **48**(1), 23–35.

27 H. E. Kissinger, *Anal. Chem.*, 1957, **29**(11), 1702–1706.

28 T. Ozawa, *Bull. Chem. Soc. Jpn.*, 1965, **38**(11), 1881–1886.

29 R. Z. Hu, S. L. Gao, F. Q. Zhao, Q. Z. Shi, T. L. Zhang and J. J. Zhang, *Thermal Analysis Kinetics*, Science Press, Beijing, 2008.

30 R. Z. Hu, and Q. Z. Shi, *Thermal Analysis Kinetics*, Science Press, Beijing, 2001.

31 R. Z. Hu, Z. Q. Yang and Y. J. Liang, *Thermochim. Acta*, 1988, **123**(88), 135–151.

32 J. R. Maccallum and J. Tanner, *Eur. Polym. J.*, 1970, **6**(6), 907–917.

33 F. Škvára and J. Šesták, *J. Therm. Anal.*, 1975, **8**(3), 477–489.

34 R. K. Agrawal, *J. Therm. Anal.*, 1987, **32**(1), 149–156.

35 T. L. Zhang, R. Z. Hu, Y. Xie and F. P. Li, *Thermochim. Acta*, 1994, **244**(244), 171–176.

36 L. C. Smith, *Thermochim. Acta*, 1975, **13**(1), 1–6.

37 R. Z. Hu, F. Q. Zhao, H. X. Gao and J. R. Song, *Fundamentals and Application of Calorimetry*, Science Press, Beijing, 2010.

38 H. J. Bruckman Jr and J. E. Guillet, *Can. J. Chem.*, 1968, **46**(20), 3221–3228.

39 M. H. Friedman, *Trans. Faraday Soc.*, 1963, **59**, 1865–1873.

40 M. H. Friedman, *Symp. Combust.*, 1963, **9**(1), 294–302.

41 R. Z. Hu, F. Q. Zhao, H. X. Gao, H. Zhao, H. A. Zhao, X. J. Wang, X. L. Zhang, F. Yu and H. X. Ma, *Chin. J. Energ. Mater.*, 2009, **17**(3), 252–254.

42 D. A. Frank-Kamenetskii, *J. Phys. Chem.*, 1939, **13**(6), 738–755.

43 W. Peng and Z. M. Du, *Chin. J. Energ. Mater.*, 2007, **15**(6), 633–636.

This journal is © The Royal Society of Chemistry 2018